

LETTER TO THE JOURNAL

Parkin deficiency promotes colorectal tumorigenesis and progression through RIPK3-dependent necroptotic inflammation

Colorectal cancer (CRC), recognized as one of the most commonly diagnosed cancers globally, is a complex disease influenced by various factors, including lifestyle, genetics, and the environment [1]. Chronic bowel inflammation is one of the primary contributors to colorectal carcinogenesis [2]. The persistent systemic inflammatory response associated with tumors contributes to cachexia and malnutrition in patient, leading to increased morbidity and mortality. Previous studies have demonstrated that Parkin acts as a negative regulator of necroptosis by binding to and polyubiquitinating RIPK3 (Receptor-Interacting Protein Kinase 3), a pivotal regulator of necroptosis [3]. Loss of Parkin promotes hyperactivation of RIPK3, necroptosis, and inflammation-driven colorectal tumorigenesis. In colitis-associated models, inhibiting RIPK3 significantly reduces pro-inflammatory cytokine expression and cancerous polyp formation. However, the role of RIPK3 in tumorigenesis is complex [4, 5], and the physiological relationship between Parkin and RIPK3 in vivo remains incompletely understood.

To further investigate the tumor-suppressive effect of Parkin through the inhibition of RIPK3 in vivo, we crossed *Prkn*^{-/-} mice and *Ripk3*^{-/-} mice to generate *Prkn/Ripk3* double-knockout (DKO) mice from heterozygous *Prkn*^{+/-} *Ripk3*^{+/-} breeding pairs [6, 7]. The DKO mice were born at the expected Mendelian frequencies and were viable, healthy, and fertile (Figure 1A). Genotyping, genome sequence and Western blot analysis of mice from each group confirmed the successful generation of *Prkn*^{-/-},

Ripk3^{-/-} and DKO (Supplementary Figure S1, Supplementary Table S1). Long-term observations revealed that *Prkn*^{-/-} mice had shorter lifespans and began to die around 8 months of age (Figure 1B). In contrast, *Ripk3* single-knockout mice and DKO mice exhibited survival curves similar to those of wide-type (WT) mice. These results indicate that Parkin deficiency may induce abnormalities that contribute to reduced survival, and this phenotype is regulated by *Ripk3*.

As reported previously [3], we found an increased frequency of rectal prolapse in *Prkn*^{-/-} mice (Figure 1C, Supplementary Figure S2A). However, in DKO mice, the number of mice with rectal prolapse significantly decreased. Meanwhile, the weight of *Prkn*^{-/-} mice was significantly less than that of WT mice (Supplementary Figure S2B). However, further knockout of *Ripk3* in *Prkn*^{-/-} mice did not rescue this low-weight phenotype. To explore this further, we dissected mice of all genotypes with similar ages and genders and found that the *Prkn*^{-/-} mice had more polyps and obvious lesion in their small intestine, while knocking out *Ripk3* in *Prkn*^{-/-} mice rescued this phenotype (Figure 1D, Supplementary Figure S2C-D). *Ripk3*^{-/-} mice developed a comparable number of polyps as WT mice. As signs of hyper-inflammation, the aged *Prkn*^{-/-} mice developed splenomegaly and had higher levels of necroptosis-related cytokines such as TNF α , IL-1 β , and IL-6 in the intestine (Supplementary Figure S2E-F). Further knockout of *Ripk3* decreased the *Prkn*-related splenomegaly and the expression of these cytokines. Collectively, these data indicate that *Prkn*^{-/-} promotes inflammation and initial hyperplasia, which can be reduced by knocking out *Ripk3*.

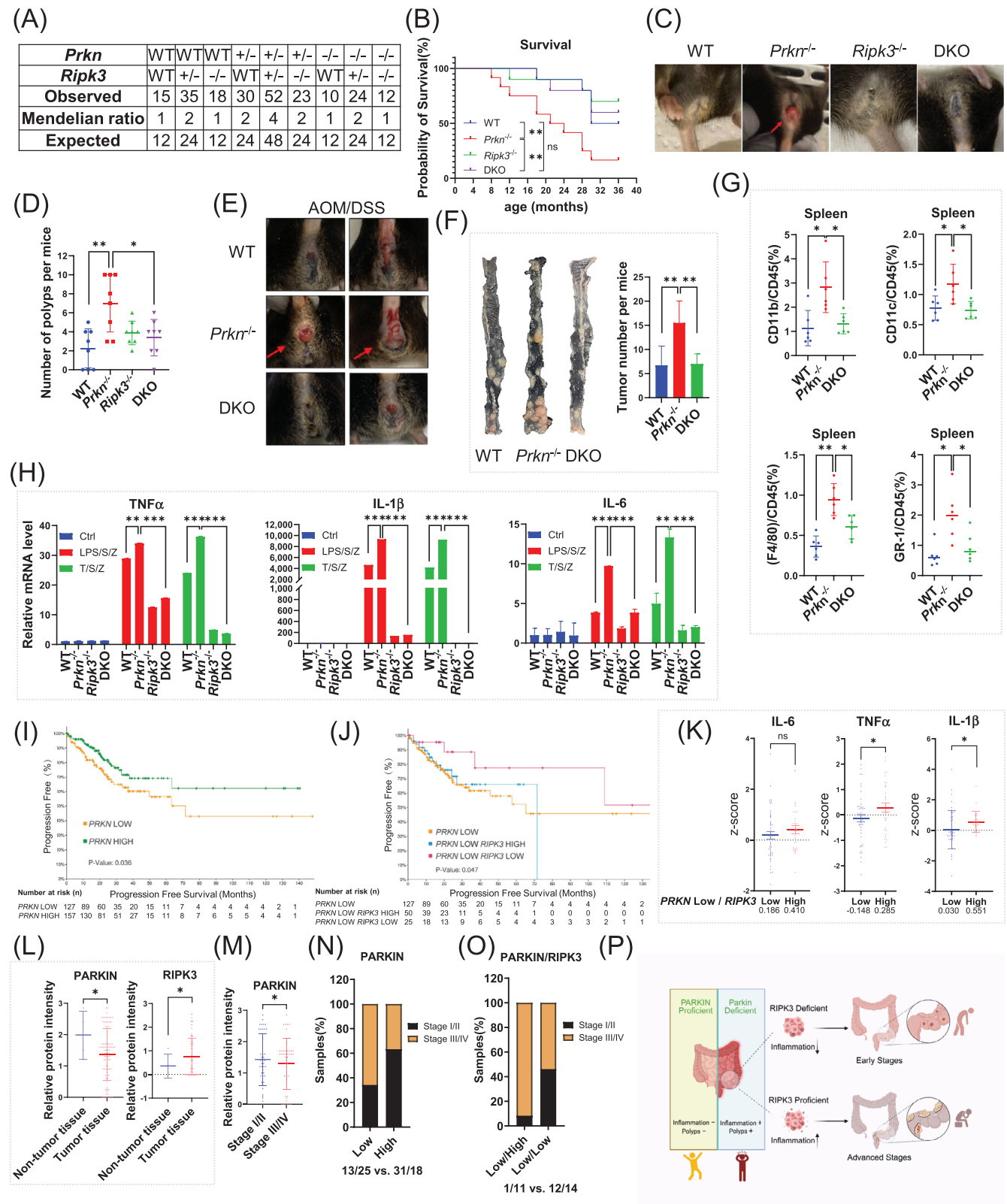
To further understand the role of Parkin in colitis-induced tumorigenesis and tumor progression, WT, *Prkn*^{-/-}, and DKO mice were subjected to AOM (Azoxymethane)-DSS (Dextran Sodium Sulfate) treatment. Mice were treated with a single intraperitoneal AOM injection followed by three cycles of 2% DSS administration

List of abbreviations: AMPK, AMP-activated protein kinase; AOM, Azoxymethane; BMDM, Bone-marrow-derived macrophage; CRC, Colorectal cancer; DKO, Double knockout; DSS, Dextran sulphate-sodium; IHC, Immunohistochemistry; MLKL, Mixed lineage kinase domain-like protein; mLNs, Mesenteric lymph nodes; PTEN, Phosphatase and tensin homolog deleted on chromosome 10; RIPK1, Receptor-Interacting Protein Kinase 1; RIPK3, Receptor-Interacting Protein Kinase 3; TCGA, The Cancer Genome Atlas.

Zheming Wu, Huaping Xiao, and Jake A Kloeber contributed equally.

This is an open access article under the terms of the [Creative Commons Attribution-NonCommercial-NoDerivs](https://creativecommons.org/licenses/by-nc-nd/4.0/) License, which permits use and distribution in any medium, provided the original work is properly cited, the use is non-commercial and no modifications or adaptations are made.

© 2025 The Author(s). *Cancer Communications* published by John Wiley & Sons Australia, Ltd. on behalf of Sun Yat-sen University Cancer Center.



in drinking water (Supplementary Figure S3A). After DSS feeding, *Prkn*^{-/-} mice demonstrated a significantly increased risk of mortality and a decrease in body weight compared to WT mice, while further knockout of *Ripk3*

in *Prkn*^{-/-} mice showed survival curves similar to WT mice (Supplementary Figure S3B-C). Finally, nearly 80% of *Prkn*^{-/-} mice exhibited rectal prolapse, a significant increase compared to WT and DKO mice (Figure 1E,

Supplementary Figure S3D). Necropsy of the entire cohort showed that colons obtained from AOM/DSS-treated *Prkn*^{-/-} mice were markedly shorter and had increased tumor burdens compared to control mice. However, this phenotype was rescued by further *Ripk3* knockout (Figure 1F, Supplementary Figure S3E-F). These results suggest that the progression of colitis-associated tumorigenesis in *Prkn*^{-/-} mice is dependent on RIPK3.

Supporting the notion that Parkin deficiency increases inflammation, we observed enlarged spleens and mesenteric lymph nodes (mLNs) in *Prkn*^{-/-} mice (Supplementary Figure S4A-B). Consistent with splenomegaly and lymphadenopathy, increased myeloid cells (CD11b⁺, F4/80⁺, CD11c⁺, Gr-1⁺) harvested from the spleen and mLNs were observed in *Prkn*^{-/-} mice compared to WT mice. However, further knockout of *Ripk3* reduced these myeloid cell populations (Figure 1G, Supplementary Figure S4C). Using cultured Bone-marrow-derived macrophages (BMDMs) in vitro, we found that *Prkn* knockout promoted TNF α (T)/SM-164 (S)/ zVAD (Z, a pan-caspase inhibitor) (TSZ) and lipopolysaccharide (LPS)/S/Z-induced necroptotic cell death. It also increased the levels of necroptosis markers, including RIPK1 (Receptor-Interacting Protein Kinase 1), RIPK3, MLKL (Mixed lineage kinase domain-like protein), and AMPK (AMP-activated protein kinase) phosphorylation [3, 8]. In contrast, necroptotic cell death and these markers were almost entirely blocked in *Ripk3*^{-/-} mice and DKO mice (Supplementary Figure S4D-E). Moreover, *Prkn*^{-/-} significantly promoted T/S/Z and LPS/S/Z-induced expression of TNF α , IL-1 β and IL-6, which was reversed

in DKO mice (Figure 1H). Collectively, these data indicate that *Prkn* knockout promotes inflammation through RIPK3-regulated necroptosis.

Given the tumor-suppressing function of *Prkn* in the AOM/DSS colorectal cancer mouse model, we investigated whether *PRKN* alterations are present in clinical specimens. A pan-cancer analysis from the The Cancer Genome Atlas (TCGA) database revealed significantly lower *PRKN* expression in various cancer types compared to adjacent tissues, especially in cancers of the digestive system, where development is closely associated with inflammation [9] (Supplementary Figure S5A). Furthermore, the colorectal cancer dataset shows *PRKN* has a similar alteration frequency to other well-known tumor suppressors, such as *PTEN* (phosphatase and tensin homolog deleted on chromosome 10) and *BRCA2* (Supplementary Figure S5B). Most of these alterations were deep deletions, supporting PARKIN's role as a tumor suppressor (Supplementary Figure S5C). Consistently, CRC patients with lower *PRKN* expression had poorer progression-free survival, along with upregulation of several inflammation-associated pathways and expression of necroptotic cytokines such as *IL-6*, *TNF α* and *IL-1 β* , mirroring the phenotypes observed in our mouse models (Figure 1I, Supplementary Figure S5D-F). Interestingly, progression-free survival curves indicate that CRC patients with lower *RIPK3* expression have better outcomes when *PRKN* expression is low (Figure 1J, Supplementary Figure S5G). A detailed analysis showed that, in patients with low *PRKN* expression but not high *PRKN* expression, lower *RIPK3* expression leads to reduced levels of IL-6,

FIGURE 1 Parkin deficiency promotes colorectal tumorigenesis and progression through RIPK3-dependent necroptotic inflammation. (A) Expected and observed genotype frequencies in offspring at weaning from intercrosses of *Prkn*^{+/-} *Ripk3*^{+/-} mice. (B) Kaplan-Meier plot of mouse survival after birth. Overall survival was tracked for 36 months. WT (*n* = 10), *Prkn*^{-/-} (*n* = 12), *Ripk3*^{-/-} (*n* = 10), DKO (*n* = 12). Statistical significance was determined using log-rank test. (C) Representative images of mice with rectal prolapse during the observation period. (D) Number of intestinal polyps in each genotype group of mice at 18 months of age. (*n* = 8 mice per group). Statistical significance was determined using Student's *t*-test. (E) Representative images of rectal prolapse in mice after AOM/DSS treatment. WT (*n* = 8), *Prkn*^{-/-} (*n* = 10), DKO (*n* = 8). (F) Representative images of colonic tumor tissues and tumor counts per colon. WT (*n* = 6), *Prkn*^{-/-} (*n* = 7), DKO (*n* = 6). Statistical significance was determined using Student's *t*-test. (G) Splenocytes were collected and analyzed by flow cytometry for myeloid cell populations stained with CD11b, F4/80, CD11c, and Gr-1 antibodies. Statistical significance was determined using Student's *t*-test. (H) mRNA extracted from primary BMDM cells was subjected to qPCR analysis. (I) Progression-free survival Kaplan-Meier curve for *PRKN* in clinical COAD samples. Statistical significance was determined using log-rank test. (J) Progression-free survival Kaplan-Meier curve for *RIPK3* in COAD samples with low *PRKN* expression. Statistical significance was determined using log-rank test. (K) Patients' samples with low *PRKN* expression were further divided into two groups based on *RIPK3* expression levels (Low: *z*-score < -1). *IL-6*, *TNF α* and *IL-1 β* expression levels were compared between these groups. Statistical significance was determined using Student's *t*-test. (L) Protein expression levels of PARKIN and *RIPK3* in non-tumor and tumor tissues. Statistical significance was determined using Student's *t*-test. (M) PARKIN protein expression in early (Stage I/II) versus advanced stages (Stage III/IV). Statistical significance was determined using Student's *t*-test. (N) Patients' samples grouped by mean PARKIN expression levels. Ratios of patient numbers in early and advanced stages were calculated and compared between groups. (O) Patients' samples with low PARKIN expression were further divided by mean *RIPK3* expression. Ratios of early- and late-stage patients were compared between groups. (P) A proposed model for PARKIN deficiency promoting colorectal cancer development and progression through RIPK3 and RIPK3-dependent inflammation. All data shown are representative of three independent experiments. ns, not significant; **P* < 0.05; ***P* < 0.01; ****P* < 0.001. Abbreviations: WT, wildtype; DKO, double knockout; AOM, azoxymethane; DSS, dextran sulphate-sodium; TNF α , tumor necrosis factor alpha; IL-1 β , interleukin-1 beta; IL-6, Interleukin-6.

TNF α , and IL-1 β , indicating a less pronounced inflammatory response (Figure 1K, Supplementary Figure S5H). Thus, our analysis of the TCGA database further supports the role of *PRKN* in colorectal cancer, demonstrating that PARKIN deficiency correlates with CRC in a manner that depends on *RIPK3* status.

Parkin deficiency has been reported to be associated with advanced tumor grade [10]. To investigate this further, we conducted a tissue microarray assay using samples from patients at different tumor stages (Supplementary Table S2). The immunohistochemistry (IHC) analysis of these tumor samples showed that PARKIN protein levels are significantly lower in cancer tissue, while RIPK3 protein levels are higher (Figure 1L, Supplementary Figure S6A-B). Samples from different tumor stages showed that PARKIN protein levels are lower in advanced stages (Stage III/IV), compared to early stages (Stage I/II), whereas RIPK3 protein levels did not exhibit significant differences between stages (Figure 1M, Supplementary Figure S6C-F). Consistent with our previous data, tumors in the low PARKIN expression cohort were more frequently observed in advanced stages (Stage III/IV) (Figure 1N, Supplementary Figure S6G). While RIPK3 expression showed no clear association with tumor stages (Supplementary Figure S6H-I), higher expression of RIPK3 was found to be associated with advanced-stage tumors (Stage III/IV) within the low Parkin expression cohort (Figure 1O). This observation aligns with the finding that combined PARKIN and RIPK3 deficiency leads to better outcomes. Taken together, these results support our hypothesis that PARKIN deficiency promotes tumor progression to advanced stages in a manner dependent on RIPK3.

In summary, our findings elucidate the role of RIPK3-dependent necroptotic inflammation in colorectal cancer induced by Parkin deficiency. Patient data reveal that poor outcomes are associated with low Parkin expression. Additionally, RIPK3 expression correlates with tumor stage progression in the Parkin-deficient cohort (Figure 1P). These results suggest new diagnostic indicators: colorectal cancer patients with low Parkin expression and high RIPK3 expression are at a higher risk of progressing to advanced stages. Early interventions are necessary for these patients to prevent tumor deterioration.

AUTHOR CONTRIBUTIONS

Zheming Wu and Zhenkun Lou conceived the project and designed all experiments. Zheming Wu performed most of the experiments and wrote the manuscript. Jake A Kloeber analyzed the TCGA data and generated the panels in Figure 5. Huaping Xiao performed the IHC staining and analyzed the data. Adrian T Ting provided the *Ripk3*^{-/-} mice pairs and provided technical expertise for the mice work. Ping Yin assisted with mice breeding and

handling. Zhenkun Lou supervised the entire project and contributed to grant support. All authors discussed the results and provided feedback on the manuscript.

ACKNOWLEDGEMENTS

We thank Dr. Vishva Dixit for generously providing the *Ripk3*^{-/-} mice. We thank Dr. SeungBaek Lee for maintaining the original *Prkn*^{-/-} mice pairs. The bioinformatics analysis of TCGA database was conducted through cBioPortal.

CONFLICT OF INTEREST STATEMENT

The authors declare that they have no competing interests.

FUNDING INFORMATION

This study was supported by National Institutes of Health funding R01CA224921. Jake A Kloeber was supported by National Institute of General Medical Sciences T32GM65841.

DATA AVAILABILITY STATEMENT

Datasets generated and analyzed in this study are available from the corresponding author upon request, in accordance with institutional data-sharing policy.

ETHICS APPROVAL AND CONSENT TO PARTICIPATE

All animal experiments were performed and monitored in strict adherence to institutional protocols, with approval from the Institutional Animal Care and Use Committee (protocol A00003886) at the Mayo Clinic, in compliance with the guidelines of the American Association for Accreditation of Laboratory Animal Care and the NIH.

Zheming Wu^{1,2}
Huaping Xiao^{1,2}
Jake A Kloeber^{1,3}
Yaobin Ouyang¹
Ping Yin¹
Jin Zhou Huang¹
Bin Chen^{1,2}
Shouhai Zhu¹
Jing Lu¹
Yiqun Han²
Xinyi Tu²
Sonja Dragojevic²
Kuntian Luo¹ 
Adrian T Ting⁴
Meng Welliver²
Zhenkun Lou¹

¹Division of Oncology Research, Department of Oncology, Mayo Clinic, Rochester, USA

²*Department of Radiation Oncology, Mayo Clinic,
Rochester, USA*

³*Mayo Clinic Medical Scientist Training Program, Mayo
Clinic, Rochester, USA*

⁴*Department of Immunology, Mayo Clinic, Rochester, USA*

Corresponding

Zhenkun Lou, Division of Oncology Research,
Department of Oncology, Mayo Clinic, 305 4th Ave SW,
Rochester, MN 55902, USA.
Email: lou.zhenkun@mayo.edu

ORCID

Kuntian Luo  <https://orcid.org/0000-0003-1938-3091>

REFERENCES

1. Siegel RL, Wagle NS, Cercek A, Smith RA, Jemal A. Colorectal cancer statistics, 2023. *CA Cancer J Clin.* 2023;73(3):233-254.
2. Terzic J, Grivennikov S, Karin E, Karin M. Inflammation and colon cancer. *Gastroenterology.* 2010;138(6):2101-2114 e5.
3. Lee SB, Kim JJ, Han SA, Fan Y, Guo LS, Aziz K, et al. The AMPK-Parkin axis negatively regulates necroptosis and tumorigenesis by inhibiting the necrosome. *Nat Cell Biol.* 2019;21(8):940-951.
4. Najafov A, Zervantonakis IK, Mookhtiar AK, Greninger P, March RJ, Egan RK, et al. BRAF and AXL oncogenes drive RIPK3 expression loss in cancer. *PLoS Biol.* 2018;16(8):e2005756.
5. Moriwaki K, Balaji S, McQuade T, Malhotra N, Kang J, Chan FK. The necroptosis adaptor RIPK3 promotes injury-induced cytokine expression and tissue repair. *Immunity.* 2014;41(4):567-578.
6. Newton K, Sun X, Dixit VM. Kinase RIP3 is dispensable for normal NF-kappa Bs, signaling by the B-cell and T-cell receptors, tumor necrosis factor receptor 1, and Toll-like receptors 2 and 4. *Mol Cell Biol.* 2004;24(4):1464-1469.
7. Goldberg MS, Fleming SM, Palacino JJ, Cepeda C, Lam HA, Bhatnagar A, et al. Parkin-deficient mice exhibit nigrostriatal deficits but not loss of dopaminergic neurons. *J Biol Chem.* 2003;278(44):43628-43635.
8. Yuan J, Ofengeim D. A guide to cell death pathways. *Nat Rev Mol Cell Biol.* 2024;25(5):379-395.
9. Chiba T, Marusawa H, Ushijima T. Inflammation-associated cancer development in digestive organs: mechanisms and roles for genetic and epigenetic modulation. *Gastroenterology.* 2012;143(3):550-563.
10. Perales-Linares R, Leli NM, Mohei H, Beghi S, Rivera OD, Kostopoulos N, et al. Parkin Deficiency Suppresses Antigen Presentation to Promote Tumor Immune Evasion and Immunotherapy Resistance. *Cancer Res.* 2023;83(21):3562-3576.

SUPPORTING INFORMATION

Additional supporting information can be found online in the Supporting Information section at the end of this article.